Adv. Opt. Techn., Vol. 1 (2012), pp. 171–180 • Copyright © 2012 THOSS Media and De Gruyter. DOI 10.1515/aot-2012-0027

Research Article

Nanostructured micro-optics based on a modified stack-and-draw fabrication technique

Mohammad R. Taghizadeh[1], Andrew J. Waddie[1,*], Ryszard Buczynski[1,2], Jedrzej Nowosielski[1], Adam Filipkowski[1] and Dariusz Pysz[2]

[1] Institute of Photonics and Quantum Sciences, School of Engineering and Physical Sciences, Scottish Universities Physics Alliance, Heriot-Watt University, Riccarton, Edinburgh, EH14 4AS, UK

[2] Glass Laboratory, Institute of Electronics Materials Technology (ITME), Wolczynska 133, 01-919, Warsaw, Poland

* Corresponding author
e-mail: A.Waddie@hw.ac.uk
Received May 4, 2012; accepted June 12, 2012

Abstract

We present the latest results in the fabrication of micro-optical components using a novel nanostructuring process. This low-cost fabrication technology, which exploits advances in the development of photonic crystal fibres, uses a modified stack-and-draw technique where macroscopic distributions of thermally and mechanically matched glasses are reduced in scale by repeated draw-down and restacking procedures until the individual glass features are significantly below the wavelength of incident light. We demonstrate that this fabrication technique is suitable for the creation of large diameter high numerical aperture micro-lenses for light collection and concentration purposes and broadband form birefringent materials.

Keywords: birefringence; diffractive optics; microlenses; micro-optics.

1 Introduction

The recent implementation of the nanostructured micro-optical element fabrication technology [1–3], based around the photonic crystal fibre stack-and-draw technique, has opened up hitherto unexplored areas of micro-optical design. In particular, areas which have required the use of costly, low volume and time-consuming fabrication methods (e.g., direct-write electron beam lithography), such as high numerical aperture 100% fill-factor microlenses and form birefringent devices, can now be explored using a conceptually simple and low cost fabrication methodology. The basic methodology behind the nanostructuring technique involves the creation of a macroscopic preform, consisting of individual thermally and mechanically matched glass rods, which is then reduced by means of a series of draw-down and restacking operations until the original glass rods are reduced to a diameter significantly below the wavelength of the incident light. At this point, incident light is no longer influenced by the individual refractive indices of the constituent glass rods but instead encounters a spatial average of the indices over the scale of around a wavelength. As the fabrication technology is based around the techniques developed for photonic crystal fibre development, it inherits all the advantages of those techniques and a single metre of drawn material can produce up to 5000 individual identical devices. In this paper, we will review the latest progress in the development of micro-optical components and investigate future directions for this novel fabrication technology. The level of optical functionality that can be achieved is, to some extent, a function of the available glasses of different refractive indices which give the designer almost arbitrary control over the performance of the optical components. Although the fabrication of the high frequency micro-structured surfaces capable of acting as 100% fill-factor fast lenses and form birefringent materials is a mature technology [4], these components have generally required the use of direct electron beam lithographic fabrication techniques, increasing the cost per unit and limiting the deployment of these components to highly specialised applications. By contrast, the nanostructuring fabrication technology allows the accurate mass duplication of the basic design for a wide range of wavelengths and applications from a single preform assembly.

2 Nanostructured micro-optic element design and fabrication

The nanostructuring process starts with the design of a structure consisting of individual glass rods with a diameter in the range of 50–500 nm drawn from a basis set of two or more soft glasses with different refractive indices and similar thermal and mechanical properties. The precise arrangement of the glasses composing this nanostructure is calculated by means of an optimisation of the desired optical properties. The small feature sizes produced by the nanostructuring procedure are sufficiently subwavelength that the algorithms developed for micro-optical components within the scalar domain are no longer applicable. A fully vectorial approach, where Maxwell's curl equations are solved numerically (using either a finite difference time domain, FDTD [5] or Fourier modal method, FMM, approach [6]), has been used successfully in the design

of several different micro-optical components. However, for the practical optimisation of these structures both the FDTD and FMM are too slow to be useful for all but the simplest of nanostructures and an alternative approach must be used. The development of effective medium theory [7], where the effective refractive index of a nanostructure is determined by a spatial average of the individual refractive indices of the constituent nanorods, gives sufficiently accurate results while allowing rapid optimisation of highly complex structures. The basic Maxwell-Garnet theory, which gives the effective permittivity of a composite structure composed of two materials [ε_m and ε_i with relative proportions of (1-δ) and δ, respectively], is expressed numerically as:

$$\varepsilon_e = \varepsilon_m \frac{\varepsilon_i(1+2\delta)-\varepsilon_m(2\delta-2)}{\varepsilon_m(2-\delta)+\varepsilon_i(1-\delta)} \tag{1}$$

where ε_i and ε_m are the relative permittivities of the inclusion and matrix materials, respectively, and δ is the proportion of inclusion material in the composite structure. This first order theory gives sufficient accuracy for the design of microlens and other non-polarisation sensitive components. For the design of polarisation sensitive components (such as form birefringent materials [8, 9]), a higher order effective medium theory which takes into account polarisation effect is needed. The second order theory suggested by Richter et al. [10] is suitable for the structures under consideration in this paper. This is expressed numerically as:

$$\varepsilon_e^{TE} = \delta\varepsilon_i + (1-\delta)\varepsilon_m + \frac{1}{3}\left(\frac{\delta(1-\delta)\Lambda\pi}{\lambda}\right)^2 (\varepsilon_i-\varepsilon_m)^2 \tag{2}$$

$$\varepsilon_e^{TM} = \frac{\varepsilon_i\varepsilon_m}{\delta\varepsilon_m+(1-\delta)\varepsilon_i} + \frac{1}{3}\left(\frac{\delta(1-\delta)\Lambda\pi}{\lambda}\right)^2 \left(\frac{1}{\varepsilon_i}-\frac{1}{\varepsilon_m}\right)^2 \left(\frac{\varepsilon_i\varepsilon_m}{\delta\varepsilon_m+(1-\delta)\varepsilon_i}\right)^2 \left[\delta\varepsilon_i+(1-\delta)\varepsilon_m\right] \tag{3}$$

where Λ is the period of the nanostructure and λ is the wavelength of illumination and the other terms are as for Eq. (1). The second order theory is only valid where $\Lambda<\lambda$ – if this condition is not satisfied a fully vectorial solution to Maxwell's curl equations must be used. Figure 1 shows a comparison between the effective refractive index ($=\sqrt{\varepsilon_e}$) predicted by the second order theory and a fully vectorial FDTD simulation for a variety of nanostructures with increasing numbers of high index material inclusions (δ). The Maxwell-Garnet theory curve lies midway between the transverse electric (TE) and transverse magnetic (TM) curves and has been omitted for the sake of clarity.

The basis set of soft glasses most commonly used in the nanostructuring process can be divided into two families, one with a low refractive index (LIC) contrast (defined in this paper as the difference between the two indices) and the other with a greater index contrast (HIC). The need for both a mechanical and thermal match between the constituent glasses is to ensure that the draw-down process is uniform across the entire structure and that no dislocations or discontinuities develop during the multistage draw-down process. In this paper, the two

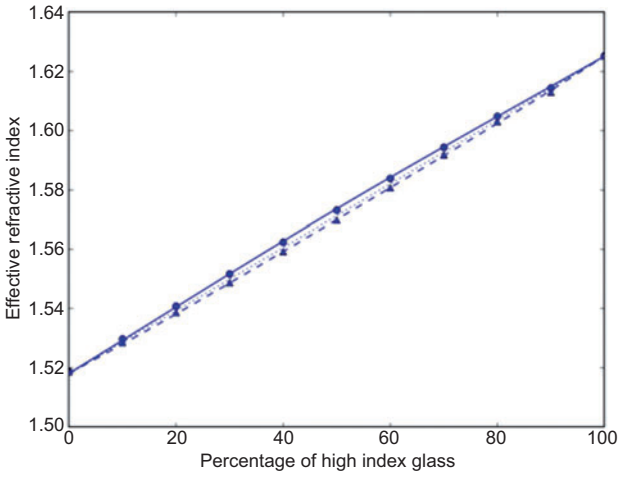

Figure 1 Variation of effective refractive index for increasing proportion of high index glass at λ=1000 nm. Circle/solid shows the second order FDTD/effective medium theory results for TE polarisation and the triangle/dashed for TM polarisation.

glasses (from the LIC family) used in the presented micro-optical components are NC21A, a novel glass developed at the Institute of Electrical Materials in Warsaw and F2, a standard off-the-shelf glass developed by the Schott Corporation. The initial preforms, created from glass rods of 0.25–1 mm diameter (with only one diameter of rod being used in a particular preform to simplify assembly), are assembled by hand to an overall preform diameter of 25–45 mm and contain between 2000 and 10 000 individual glass rods. This limits the overall size of the final nanostructured element to the 20 µm to 200 µm range. After initial preform assembly, the structure is drawn-down in a fibre-drawing tower to an intermediate preform diameter of 1–2 mm. The intermediate preforms are then cut to a length of 0.5–1 m and restacked with uniform glass rods to form a secondary preform, of similar diameter to the initial preform, which is then drawn-down to a final diameter of 1 mm. This final diameter corresponds to individual features of between 50 and 200 nm giving a fabricated component suitable for use under visible and near-infrared (0.5–2 µm) illumination. The diameter uniformity of the glass rods used in the preform assembly is, to some extent, unimportant as due to the large overall draw-down used in the fabrication process (~1000–10 000), any slight discrepancies in the glass rods will generally be smaller than the boundary diffusion lengths of the constituent glasses and have thus been taken into account in the effective medium design algorithm. Figure 2 shows a schematic of the different stages of the nanostructuring procedure – the individual stages corresponding to (a) initial preform assembly, (b) initial draw-down, (c) intermediate preform assembly, (d) secondary draw-down and (e) final dicing and polishing. It should be noted that stages (c) and (d) can be repeated as necessary to ensure that the final feature sizes reach the desired dimensions. The final diameters of the fabricated optical components (using this basic fabrication technique) lie in the 5 µm–20 µm range with effective f-numbers down to f/1 having been observed with diffraction limited optical performance [1–3].

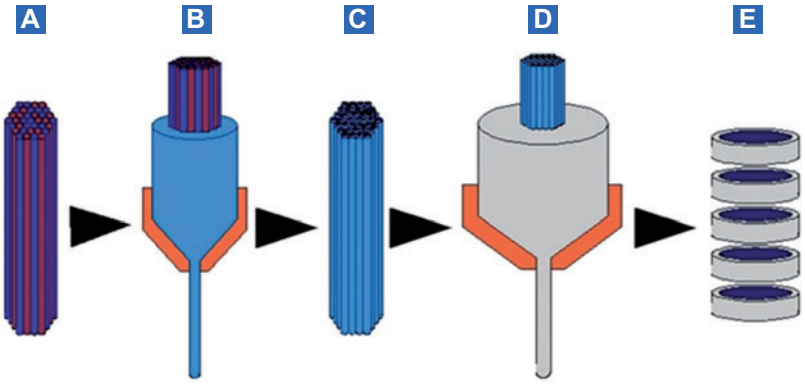

Figure 2 Schematic of stack-and-draw process for nanostructured micro-optics fabrication.

3 Large diameter nanostructured microlenses

The nanostructured microlens fabrication technology, which exploits the effective medium approach described above, is capable of producing very small diameter (<20 μm), very fast (f/#≤1.5) lenses with diffraction limited performance [1, 2]. However, it should be noted that these microlenses were fabricated using conventional preform assembly techniques, where individual rods (~10 000 for a 20 μm lens) of the basis glasses are placed in the appropriate pattern. Use of this technique to assemble a larger diameter microlens (say 100 μm diameter) is not feasible, as it would require the manual placement of 100 000–250 000 individual glass rods. Although the advent of robotic preform assembly methods may make this direct nanostructuring approach practical in the future, we have adopted an alternative approach to the fabrication of large diameter nanostructured microlenses which combines the overall flexibility of the nanostructuring technology with the large diameter capabilities of a Fresnel zone plate approach. The large diameter nanostructured lens was created using a hexagonal lattice of 100×100 nanostructured rods (metarods) ordered as shown in Figure 3. Each of the metarods has a diameter of 1.2 μm and is composed of 50×50 rods of 20 nm diameter. There are seven different types of metarod (Figure 4) composed of different fractions of the glasses (NC21 and F2) to obtain an effective refractive index variation and the effective refractive indices of the metarods shown in Figure 4 are linear between n1=1.5212 (pure NC21 glass) and n7=1.6068 (pure F2 glass). NC21 is a silicate glass synthesised in-house at the Institute of Electronic Materials Technology (ITME) in Warsaw (n_{dNC21}=1.5212).

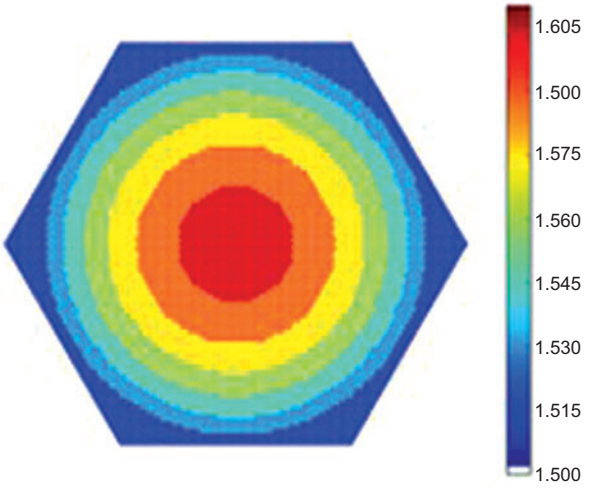

Figure 3 Layout of 100×100 hexagonally packed metarods for seven level nanostructured microlens.

Figure 5 shows the assembly of the large diameter nanostructured microlens at various stages of the complete assembly process. The final thickness of the cut and polished sample was 140 μm compared to a calculated lens quarter pitch of the nanostructured microlens of 249 μm. Simulations of the focusing behaviour of the fabricated lens design show that a sample thickness of 140 μm gives a lens working distance of 65 μm and a focal spot diameter of 0.9 μm at 850 nm and a working distance of 60 μm and a focal spot diameter of 0.6 μm at 633 nm.

The final cut and polished microlens was placed within the experimental apparatus shown in Figure 6A – this setup is used to determine the front surface of the lens and then, by micro-stepping back from this plane, an observation of the focal plane can be made.

Figure 6B shows an image of the front surface of the nanostructured lens under 633-nm illumination and allows the overall diameter of the lens to be determined. It should be noted that there is a large degree of error associated with this measurement, both from the precise determination of the front surface and the measurement of the overall diameter of the lens. The focal length of the fabricated microlens was determined for two different wavelengths (633 nm and 850 nm) to verify that the microlens is capable of diffraction limited focusing behaviour over a relatively large wavelength range. It can be seen from Figures 7 and 8 that this prediction is generally correct – there is a slight discrepancy between the measured and calculated working distances. The observed working distances are approximately 50% smaller that those predicated by theory. This is due to the accuracy of our measurement system and the difficulties associated with precisely determining the surface and total diameter of the lens – a process which is more complicated for the infrared wavelength measurements and accounts

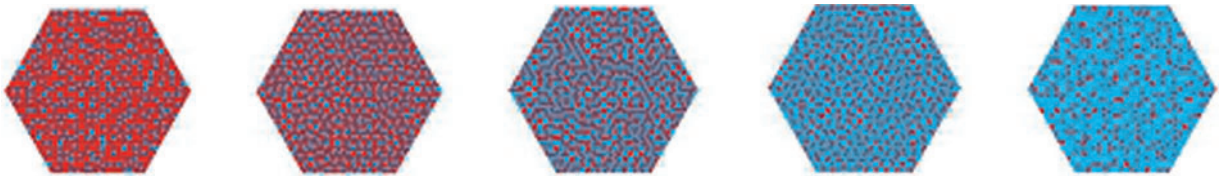

Figure 4 Structures of five metarods composed of two fundamental glasses NC21 and F2 according to the calculated pseudorandom pattern to ensure a uniform effective refractive index within each of the five nanostructured rods.

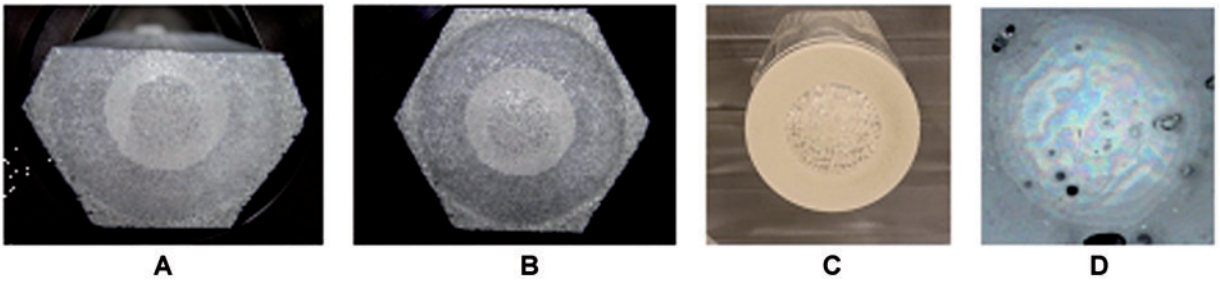

Figure 5 Development of nanostructured quantised GRIN lens: (A) assembly of preform with metarods, (B) final preform of lens structure with a diameter of 60 mm, (C) intermediate preform with a diameter of 30 mm and (D) final microlens with a diameter of 0.1 mm.

for the larger apparent discrepancy between the simulations and experimental results. By assuming we have a systematic error in the measurement of the working distance as well as in the measurement of the overall lens diameter, the difference in working distances obtained for both the 633 nm and 850 nm illuminations are in good agreement with predicted values.

4 Nanostructured form birefringence

The point of maximal effective refractive index difference in Figure 1 corresponds to a 50/50 high/low index structure and is ideally suited to the creation of a form birefringent material. It consists of alternating slabs of high and low refractive index glass with the direction of variation lying perpendicular to the direction of propagation as shown in Figure 9A.

The initial preform (Figure 9B) of this structure was assembled from 1 mm diameter rods of the constituent glasses and the simple design results in a considerably simplified preform assembly stage when compared to that required by the nanostructured lens designs. Furthermore, the final index variation scale is on the order of one-half to a quarter of the incident illumination resulting in a much reduced draw-down requirement for this material compared

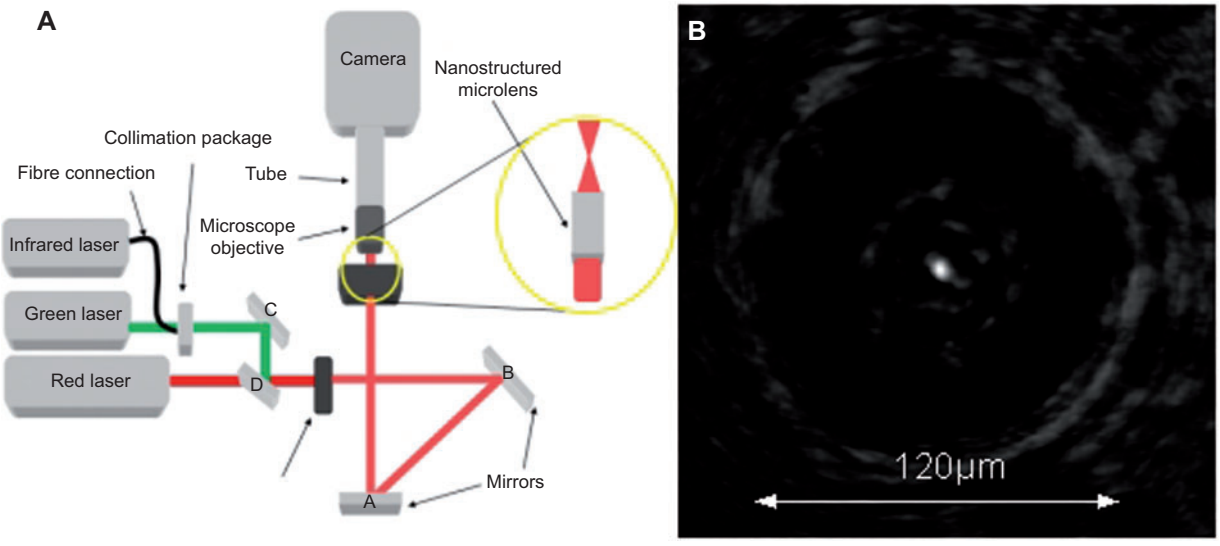

Figure 6 Measurement setup (A). Typical output image of the measured lens imaged at the lens focus captured by linear CCD camera (B). Scattering at lens border can be observed.

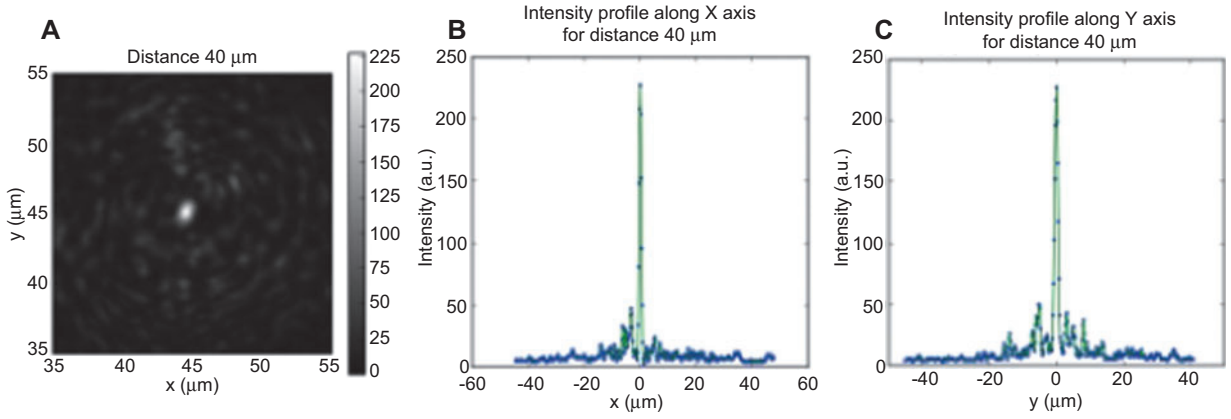

Figure 7 Intensity distribution and cross-sections in x and y in the focal plane at a working distance of 40 µm at a wavelength of 633 nm.

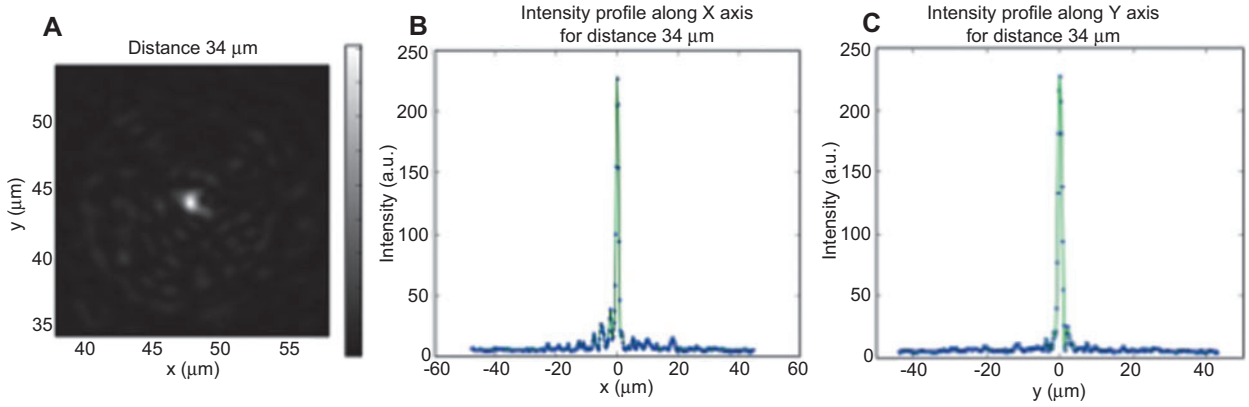

Figure 8 Intensity distribution and cross-sections in x and y in the focal plane at a working distance of 34 µm at a wavelength of 850 nm.

to that required for the nanostructured microlens where the final index variation scale is on the order of one-tenth to one-twentieth of the incident illumination. The refractive index dispersion of the low index contrast glasses in the modelled nanostructures is given by the Sellmeier coefficients shown in Table 1.

To determine the final index variation scale of the artificially birefringent material, the variation in the birefringence or difference between the TE and TM polarisation refractive indices (given here by Δn) as a function of the overall period of the nanostructure was studied by means of an FDTD simulation for several different wavelengths of incident light (500 nm, 1000 nm, 1500 nm and 2000 nm). The results of this study are shown in Figures 10 and 11 – each curve in Figure 11 has been scaled by the peak value of Δn given in Figure 10. From Figure 10, the second order effective medium theory (solid blue) shows good agreement with the fully vectorial results (blue dots). An inverse wavelength fit (green) to the simulated Δn shows constant birefringence over 300 nm wavelength bands.

It can be seen from Figure 11 (where the plotted Δn are scaled relative to the peak Δn from Figure 10) that for each

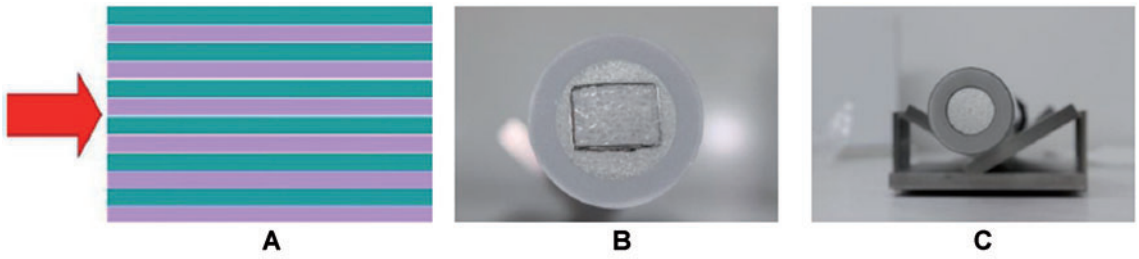

Figure 9 (A) Basic nanostructured birefringent device design composed of two soft glasses. (B) Initial perform. (C) Intermediate preform prior to final draw-down.

Table 1 Sellmeier coefficients for low index contrast glass family.

Name	B1	B2	B3	C1	C2	C3
F2	1.34533	0.20907	0.93735	0.009977	0.047045	111.88676
NC21A	0.64711	0.64711	98.02462	0.008915	0.008915	12678.084

wavelength, there is a definite threshold beyond which the expected level of birefringence is significantly reduced. This reduction in Δn is due to the structure ceasing to operate as a true effective medium and instead beginning to function as a scalar domain diffraction grating – as shown by the inset figures for an incident wavelength of light of 1000 nm. In each of the inset figures the structure is a set of three periods of the high-low index structure with the direction of variation running across the inset figure as shown in Figure 12 for the 1.5 period/wavelength inset figure.

The final choice of test structure was driven by the need to ensure a period of significantly less than the wavelength of illumination without entering the lower wavelength region where the calculated birefringence is not constant over a large wavelength range. The target period was set to 1 μm for an illumination wavelength of 1550 nm (allowing operation as low as 1200 nm without compromising the second order effective medium limitation). The initial preform (Figure 9B) consisted of a rectangular 'active' area held in place by a metal foil inside a cylindrical tube of NC21A with appropriate spacing rods to fill any air gaps in the structure. The metal foil which will have a thickness of ~10 nm after the full draw-down process has a minimal effect on the observed birefringence of the final component. After initial draw-down, the resulting 1 mm diameter cane was placed within another NC21A cylindrical tube (Figure 9C) and the final draw-down processing performed. The final dimensions of the 'active' area were measured as 39.6 μm×27.3 μm with a total component diameter of 1.7 mm.

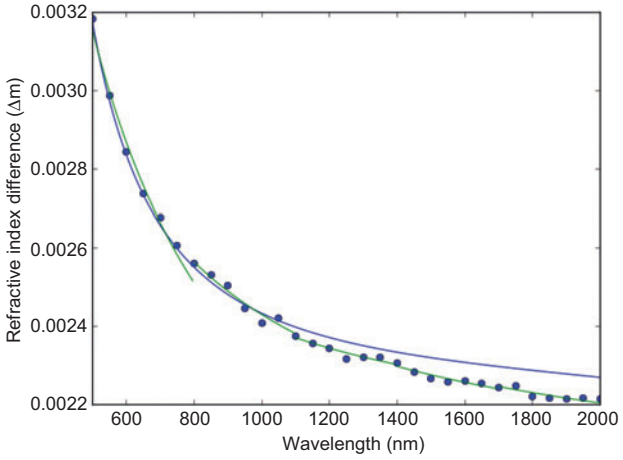

Figure 10 Variation of peak birefringence with wavelength for 250 nm period material.

The birefringence of the fabricated sample was measured using a modified version of the method proposed by Robertson [11] which enables the retardation of the test sample to be determined in a straightforward manner. The basic experimental setup is shown in Figure 13 and the measurement of the angle on the output polariser which gives a minimum for each combination of input polarisation state and quarter wave place angle can be used to determine the overall retardation of the test sample.

The angle of the test sample was held constant throughout these measurements although, in principle, an identical set of measurements could be performed for several different test sample orientations. A simulation of the measurement system, implemented using Jones matrices [12] for each of

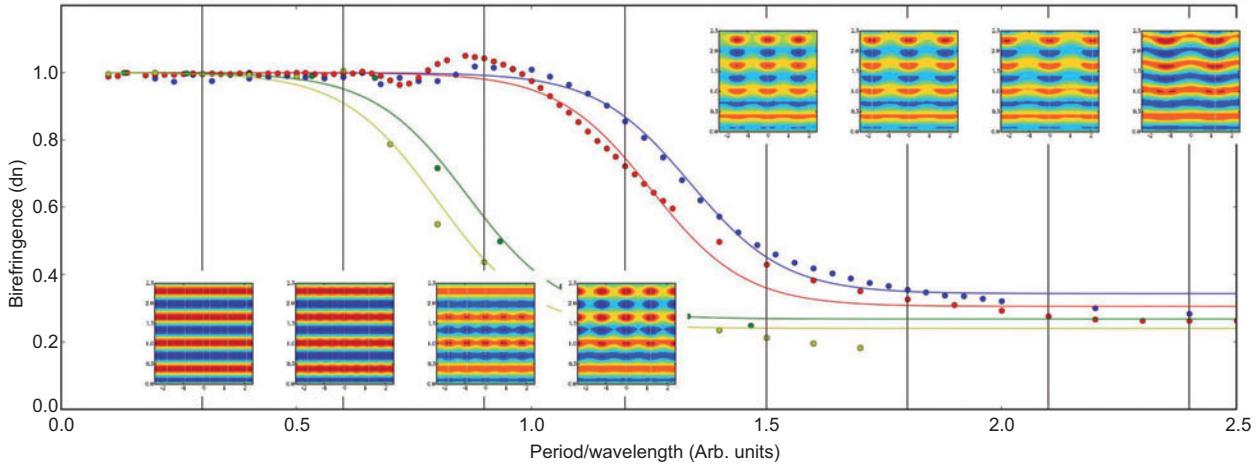

Figure 11 FDTD simulations of nanostructured birefringent material for different wavelengths (500 nm: yellow, 1000 nm: green, 1500 nm: red, 2000 nm: blue). Inset images are electric field magnitudes within the structure-propagation direction up the page.

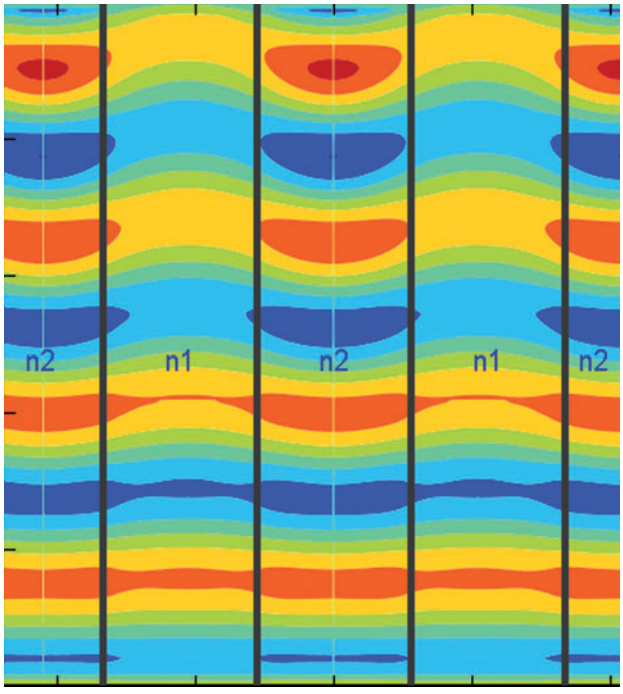

Figure 12 Structure of birefringent material for period/wavelength=1.5 inset figure from Figure 11. n2>n1.

the components in the experimental setup, the variation of the output polariser angle (θ) that produces a minimum intensity on the detector with quarter wave plate angle (ω) has the general form shown in Figure 14.

The measured minimum intensity polarisation angle from the test sample is also shown in Figure 14 and it can be seen that it generally follows the curve of the modelled system. The relatively small discrepancies between the modelled and experimental results for the lower curve are primarily due to the difference in the relative proportions of the two input polarisations in the lower experimental curve (210 μW:17 μW) compared to the relative proportions in the upper experimental curve (0.84 μW:227 μW). The larger admixture of the non-desired polarisation slightly shallows the leading edge while adding a small overall shift to the minimum angle.

A gradient descent numerical fit using the Jones calculus is not possible due to the presence of the minimum function in the determination of the output polarisation angle. A plot of the maximum differential with respect to the QWP angle (ω) of the difference between the minimum angles of the two orthogonal polarisations gives a monotonic (over a range of QWP angles between 0 and π radians) function with distinct differences between different relative area measurements. The peak angular differential metric is calculated by:

$$\Lambda_p^{\alpha} = \max_{\omega \in [0\pi]} \frac{d(\theta_{p1} - \theta_{p2})}{d\omega}$$

where $p1$ and $p2$ are the two polarisations shown by the solid/triangle and dashed/circle lines, respectively, in Figure 13. A plot of this metric is shown in Figure 15 with the measured peak differential (and the determined error bounds on the measurement) shown by the horizontal blue lines.

From Figure 15, the measured level of retardation for the test sample lies either between 0.6 and 1.0 radians or between 5.3 and 5.7 radians – the rotational mounts used in the measurement were accurate to ±1° and the use of more accurate rotational mounts for the quarter wave plate and the output polariser would reduce the relatively large errors in the peak angular differential. The total thickness of the test sample used in the experiment was 10.77±0.05 mm giving a predicted phase retardation from the effective medium theory derived refractive indices of 2.287 radians. This value appears to be significantly different from that calculated from the experimental data; however, due to the non-determined rotation of the sample relative to the input polarisation

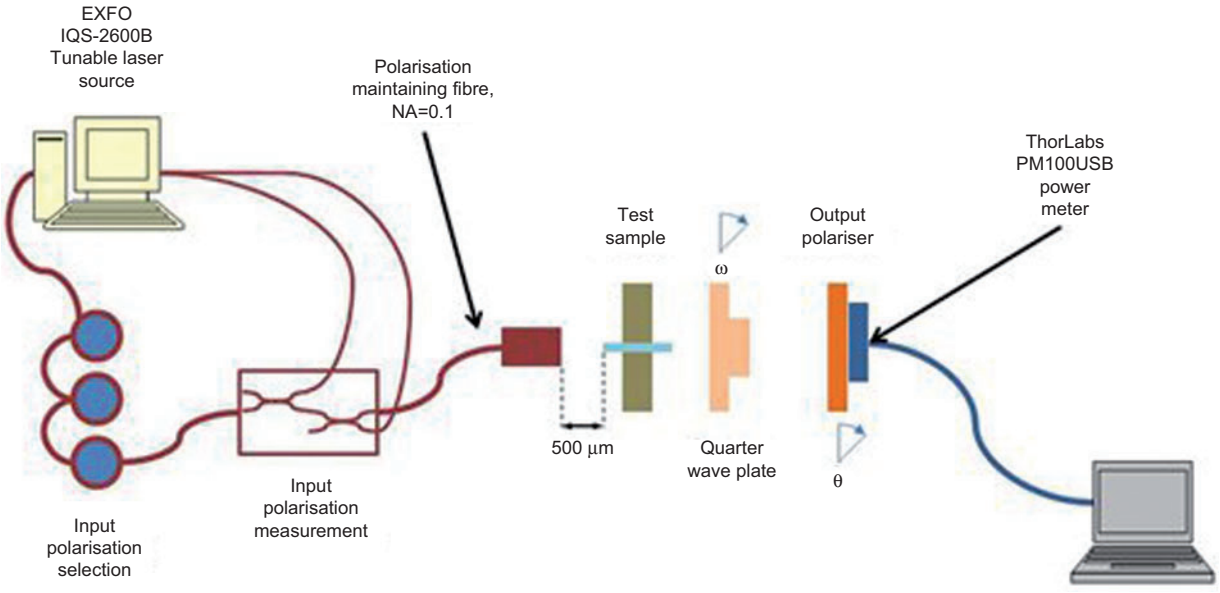

Figure 13 Experimental set-up used to determine retardation of fabricated nanostructured birefringent material.

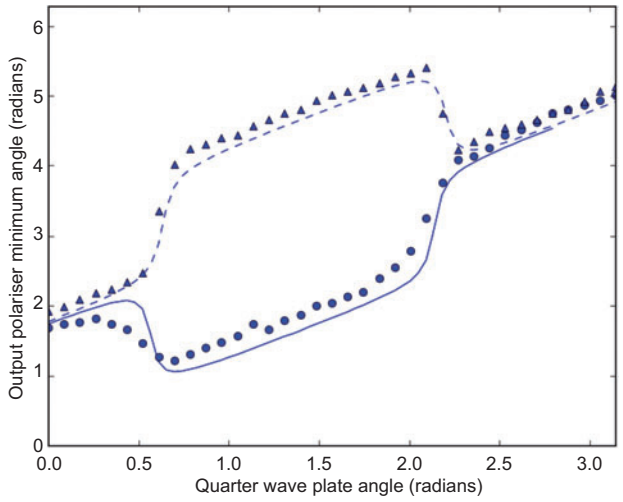

Figure 14 Comparison between modelled and experimental variation of minimum intensity polarisation angle with QWP angle for two approximately orthogonal polarisations (θ_{solid}=97°, θ_{dashed}=171°, θ_{circle}=105°, $\theta_{triangle}$=18°).

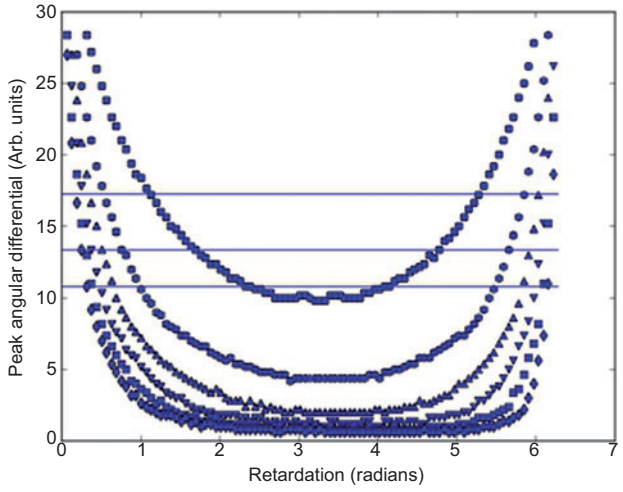

Figure 15 Variation of peak angular differential for different relative areas (circle, 0.05; hex, 0.10; up triangle, 0.15; down triangle, 0.20; square, 0.25; diamond, 0.30).

angles, an increase (or decrease) in the derived retardation of π radians can be made without loss of generality. This brings the calculated value of the retardation of the test sample to 5.429 radians which lies within the error bounds for the derived result.

5 Conclusions

Nanostructured micro-optics, produced using the modified stack-and-draw technique, are capable of a wide range of optical functionalities. We have successfully demonstrated the creation of large diameter, high numerical aperture (NA) microlenses and customised birefringent materials using the same conceptually simple fabrication method. Furthermore, although we have demonstrated only two example structures, the nanostructuring method is capable of producing any arbitrary two-dimensional refractive index distribution and can, in principle, be used to fabricate any micro-optical component with feature sizes ranging down to the subwavelength regime. One significant advantage of the nanostructuring technology outlined in this paper is that a single preform can be used to generate a large number of identical (on the scale of the incident light) micro-optical devices which can be scaled to different sizes by simply changing the draw-down factor of the final draw stage. This mass duplication behaviour can be seen in Figure 16, which shows three separate devices fabricated from the same preform and cut from sections of the drawn preform with a separation of 10–20 m. The overall diameter of each of the microlenses is 100 μm.

The focusing behaviour of the large diameter microlenses fabricated using this technique closely matches that predicted by gradient index optics theory. Furthermore, the nanostructuring technology allows the fabrication of non-spheric refractive index profiles, opening the way for the creation of non-standard microlenses as well as more general diffractive optical structures. The polarisation selectivity of the nanostructured components, which can be achieved using a very simple preform pattern, suggests the creation of multifunctional elements which can be precisely tailored to the application. The fabricated form birefringent material exhibits uniform birefringence over a wide range of wavelengths and, when combined with the achromatic behaviour observed with

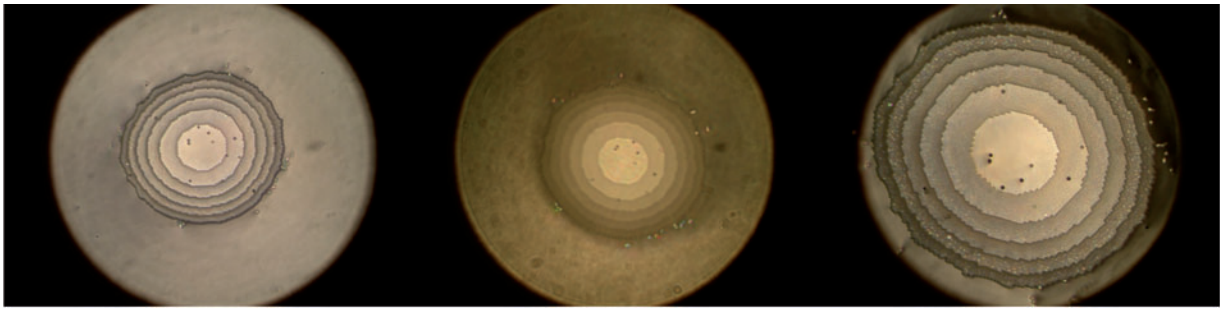

Figure 16 Nanostructured microlenses drawn from the same base preform. The spatial separation of each of the microlens sections is between 10 and 20 m.

the microlenses, would permit the development of broadband micro-optical assemblies for, e.g., increased light gathering in single photon counting applications [13].

References

[1] F. Hudelist, R. Buczynski, A. J. Waddie and M. R. Taghizadeh, Opt. Expr. 17, 3255–3263 (2009).
[2] F. Hudelist, J. M. Nowosielski, R. Buczynski, A. J. Waddie and M. R. Taghizadeh, Opt. Lett. 35, 130–132, (2010).
[3] J. M. Nowosielski, R. Buczynski, F. Hudelist, A. J. Waddie and M. R. Taghizadeh, Opt. Comm. 283, 1938–1944 (2010).
[4] H.-P. Herzig, in 'Micro-optics: Elements, Systems and Applications' (Taylor and Francis, London, 2007).
[5] A. Taflove and S. C. Hagness, in 'Computational Electrodynamics. The Finite Difference Time-Domain Method', 3rd ed. (Artech House, Boston, MA, 2005).
[6] P. Lalanne, JOSA A, 14, 1592–1598 (1997).
[7] A. Sihvola, in 'Electromagnetic Mixing Formulas and Applications' (The Institution of Electrical Engineers, London, 1999).
[8] D. C. Flanders, Appl. Phys. Lett. 42, 492–494 (1983).
[9] A. J. Waddie, R. Buczynski, F. Hudelist, J. Nowosielski, D. Pysz, et al., Opt. Mat. Expr. 1, 1251–1261 (2011).
[10] I. Richter, P.-C. Sun, F. Xu and Y. Fainman, Appl. Optics 34, 2421–2429 (1995).
[11] S. R. M. Robertson, Appl. Optics 22, 2213–2216 (1983).
[12] R. C. Jones, JOSA, 31, 488–493 (1941).
[13] S. Donati, G. Martini and E. Randone, J. Lightwave Tech. 29, 661–665 (2011).

M. R. (Mo) Taghizadeh is Professor of Physics and Head of Diffractive and Micro-Optics Group at the Institute of Photonics and Quantum Sciences (IPaQS), School of Engineering and Physical Sciences, Heriot-Watt University in Edinburgh, UK. He received his BSc, MSc and PhD in 1977, 1978 and 1982, respectively. He has published around 300 papers in the peer refereed journals and/or at international conferences and holds several patents in the areas of nano-structured optics and diffractive and micro-optical elements. Professor Taghizadeh has chaired numerous committees and international conferences including those organised by the Optical Society of America, the European Optical Society and SPIE.

Andrew Waddie received his Ph.D. in Optoelectronic Neural Networks from Heriot-Watt University in 1996. Since then he has been a post-doctoral researcher in the Diffractive and Micro-Optics Group at Heriot-Watt. His research interests include the design and fabrication of diffractive micro-optical elements, the development of novel micro-optical fabrication techniques and the simulation of electromagnetic wave interactions with micro- and nanostructured materials using both the Finite Difference Time Domain and Angular Spectrum of Plane Waves methods.

Ryszard Buczynski received the Ph.D. degrees in physics and in applied sciences in 1998 and 1999 from Warsaw University of Technology, Poland and Vrije Universiteit Brussel, Belgium, respectively. Since 2002 he has been an assistant professor at the Faculty of Physics, University of Warsaw, Poland. His research interests include modeling, characterization and application of microstructured fiber, photonic band gap materials and micro optics.

Jędrzej Nowosielski was awarded an M.Sc. in physics within the framework of Individual Inter-Faculty Studies in Mathematics and Natural Sciences at the University of Warsaw. His masters thesis concerned the coupling of polymer waveguides fabricated using a direct laser writing technique. At present he is a PhD student at Heriot-Watt University in Edinburgh and also at the University of Warsaw. He is working in a joint project related to nano- and micro-structured optical elements including GRIN microlenses, DOEs, and birefringent materials fabricated with stack-and-draw technique

Dariusz Pysz received his Eng and MSc degrees in technical physics (optics) from Warsaw University of Technology in 1985. Currently he is a research scientist in the Glass Laboratory of the Institute of Electronic Materials Technology. He has participated in State Committee for Scientific Research (Poland) R&D projects and many ITME R&D projects (light- and image-guide fiber optic integrated rods, flexible capillaries, tapered optical fibers, multi-capillary structures, photonic crystal fibers). His primary research interests are photonic crystal fibers and fiber optic nanostructures. He is author and coauthor of more than 100 publications in journals and scientific papers presented at conferences.